

A quantum limit to non-equilibrium heat engine performance imposed by strong system-reservoir coupling

David Newman,^{1,2} Florian Mintert,¹ and Ahsan Nazir²

¹*Department of Physics, Imperial College London, London, SW7 2AZ, UK*

²*School of Physics and Astronomy, The University of Manchester, Oxford Road, Manchester, M13 9PL, UK*

(Dated: June 24, 2019)

We show that non-vanishing system-reservoir coupling imposes a distinct quantum limit on the performance of a non-equilibrium discrete stroke quantum heat engine operating in finite time. Even in the absence of quantum friction along the isentropic strokes, finite system-reservoir coupling induces correlations that result in the generation of coherence between the energy eigenstates of the working system. This coherence acts to hamper the engine's power output as well as the efficiency with which it can convert heat from the reservoir into useful work output, and cannot be captured by a standard Born-Markov analysis of the system-reservoir interactions. Despite this, we find that a strongly coupled engine can generate a greater power output than its weakly coupled counterpart, which can be boosted by additional dephasing to rid the engine of coherence.

I. INTRODUCTION

Heat engines that operate in the quantum regime have formed the basis for many theoretical studies within the last few years [1–13]. It is well understood that finite time quantum engines operating outside the adiabatic regime are hampered by coherence that develops between the energy eigenstates of the working system during the work extraction strokes [14, 15]. This effect, known as quantum friction, degrades the engine's work output when compared with an engine where work strokes are performed infinitely slowly such that the quantum adiabatic theorem holds. Avoiding the costs imposed by quantum friction, negating this quantum disadvantage, may be possible by employing techniques known as shortcuts to adiabaticity, which enable the engine work strokes to remain adiabatic despite being carried out in finite time [16, 17], or through quantum lubrication by means of an appropriate form of environmental noise [18]. Nevertheless, quantum coherence accrued through non-adiabatic work strokes can prove to be advantageous when comparing instead with the equivalent non-adiabatic stochastic (classical) engines in the particular limit of small action discussed in Refs. [19, 20]. Away from this limit, however, it has been argued that coherence reverts to acting as a disadvantage over the classical non-adiabatic case [21]. With nanoscale heat engines no longer simply the preserve of theoretical studies, recent experimental realisations [15, 22, 23] and observations of the effects of quantum coherence in the laboratory [24] act as urgent motivation for studies of this regime of coherent engine operation.

Here we discuss the effects of system-reservoir correlations accrued during heat exchange strokes in a quantum engine consisting of a two-level system (TLS) coupled to bosonic reservoirs, operating in a finite time version of the Otto cycle. In typical treatments of the quantum Otto cycle, a weak coupling assumption is made which results in system and environmental reduced quantum states remaining uncorrelated at all times. In the adi-

abatic regime, where no coherence accrues in the TLS during the work extraction strokes, the weak coupling assumption also means the TLS reduced state remains diagonal in its energy eigenbasis during the heat exchange strokes. By going beyond the weak coupling assumption, but remaining adiabatic along the work extraction strokes, we shall see how system-environment correlations lead to performance losses even where quantum friction plays no role, constituting a distinct quantum limit.

II. MODEL AND METHODOLOGY

A. The Otto cycle model at finite time

In order to access the strong coupling regime we make use of the reaction coordinate (RC) formalism, which involves a unitary mapping of the Hamiltonian describing the system, reservoirs and their interaction to one which defines a collective coordinate for each reservoir and its interaction with the system [25–27]. It is especially useful in the context of (quantum) thermodynamic cycles where system-reservoir interactions are non-negligible [28–30]. We shall employ here only the features of this mapping which are salient to the present analysis of the finite time Otto cycle and refer the reader to these references for more in depth discussion of the method itself.

We consider a TLS which may interact separately with two heat reservoirs, at temperatures T_h and T_c with $T_h > T_c$. The protocol for the Otto cycle consists of four strokes which we label using eight points $A'BB'CC'DD'A$: *Hot isochore*: at A' the TLS is coupled to the hot reservoir and interacts with it for a time τ_i to reach B . The interaction between the TLS and the hot reservoir is then instantaneously set to zero and we label this point B' ; *Isentropic expansion*: The self-Hamiltonian of the TLS, H_S , is tuned such that the gap between the two energy eigenvalues is reduced. The time taken for this stroke is given by τ and we label as C the

point at which the desired energy gap has been set. Now, the interaction between the TLS and the cold reservoir is switched on at point C' ; *Cold isochore*: The TLS interacts with the cold reservoir at temperature T_c for a time τ_i , to reach point D . The system is then decoupled from the cold reservoir to reach point D' ; *Isentropic compression*: H_S is tuned for a time τ such that the gap between energy eigenstates is increased back to the same level as at point A' , reaching point A . The cycle is completed by instantaneously turning on the interaction with the hot reservoir at point A' . These strokes are repeated until a limit cycle is reached [31]. Once in this limit, the global quantum state at any particular point in the cycle is the same from one cycle to the next.

The full Hamiltonian for the internal energy of the TLS and the two reservoirs plus interaction terms reads

$$H(t) = H_S(t) + H_{R_h} + H_{R_c} + H_{I_h} + H_{I_c}, \quad (1)$$

where each term is given by

$$H_S(t) = \frac{\epsilon(t)}{2}\sigma_z + \frac{\Delta(t)}{2}\sigma_x, \quad (2)$$

$$H_{R_h} = \sum_k \omega_k^h b_k^\dagger b_k, \quad (3)$$

$$H_{R_c} = \sum_q \omega_q^c c_q^\dagger c_q, \quad (4)$$

$$H_{I_h} = -\sigma_z \sum_k f_k^h (b_k^\dagger + b_k), \quad (5)$$

$$H_{I_c} = -\sigma_z \sum_q f_q^c (c_q^\dagger + c_q). \quad (6)$$

We have used the notation σ_z and σ_x for the well-known Pauli Z and X operators acting on the TLS subspace. The TLS bias and tunneling are denoted respectively by $\epsilon(t)$ and $\Delta(t)$ where the time dependence arises over the isentropic strokes when these parameters are tuned to either increases or decreases the splitting between the energy eigenlevels of $H_S(t)$. This splitting is given by $\mu(t) = \sqrt{\epsilon(t)^2 + \Delta(t)^2}$ and, in particular, we will need to know the values of μ during the hot stage or cold stage of the cycle, which we label with a subscript as μ_h and μ_c , respectively. Annihilation operators for excitations at frequencies ω_k^h and ω_q^c in the hot and cold reservoirs are given respectively by b_k and c_q , which satisfy bosonic commutation relations. The reservoir oscillators couple to the TLS via H_{I_h} and H_{I_c} with strengths f_k^h and f_q^c , and we note that the two interaction terms are only present during either the hot or cold isochores, when the TLS is interacting with the relevant reservoir.

Standard treatments of Otto cycle heat engines invoke the weak coupling assumption, i.e. that the two interaction terms are (negligibly) small. This leads to a tractable analysis in terms of a quantum state describing the TLS and reservoirs which remains in tensor product form at all times. In the finite coupling regime where the interaction terms cannot be neglected, it is a more involved task to compute the state (which in general is

not in tensor product form) at various points around the cycle. In order to access this regime, we extend the RC formalism (as described in Refs. [26, 27]) from the infinite time Otto cycle considered in Ref. [28], to inherently non-equilibrium finite time cycles. In this approach, the reservoir contribution to the hot interaction term in Eq. (1) is mapped to a single collective mode (the RC) such that

$$H_{I_h} = -\sigma_z \sum_k f_k^h (b_k^\dagger + b_k) = -\lambda_h \sigma_z (a_h^\dagger + a_h), \quad (7)$$

where a_h^\dagger creates an excitation in the RC mode for the hot reservoir with natural frequency Ω_h , and a_h^\dagger , a_h satisfy bosonic commutation relations as long as $\lambda_h = \sqrt{\sum_k f_k^h}$. The hot reservoir Hamiltonian becomes

$$H_{R_h} = \Omega_h a_h^\dagger a_h + \sum_k g_k^h (a_h^\dagger + a_h) (r_k^{h\dagger} + r_k^h) + \sum_k \nu_k^h r_k^{h\dagger} r_k^h, \quad (8)$$

while the system Hamiltonian remains unchanged. Here, the creation operator $r_k^{h\dagger}$ creates an excitation at frequency ν_k^h in an oscillator belonging to a redefined residual reservoir which interacts weakly with the hot RC mode via couplings g_k^h . Similar equations hold for the cold reservoir and cold interaction term. The full Hamiltonian thus becomes

$$H(t) = H_{S'}(t) + H_{R'_h} + H_{R'_c}, \quad (9)$$

where we have made the following definitions:

$$H_{S'}(t) = \frac{\epsilon(t)}{2}\sigma_z + \frac{\Delta(t)}{2}\sigma_x - \lambda_h \sigma_z (a_h^\dagger + a_h) - \lambda_c \sigma_z (a_c^\dagger + a_c) + \Omega_h a_h^\dagger a_h + \Omega_c a_c^\dagger a_c, \quad (10)$$

$$H_{R'_h} = \sum_k g_k^h (a_h^\dagger + a_h) (r_k^{h\dagger} + r_k^h) + \sum_k \nu_k^h r_k^{h\dagger} r_k^h, \quad (11)$$

$$H_{R'_c} = \sum_q g_q^c (a_c^\dagger + a_c) (r_q^{c\dagger} + r_q^c) + \sum_q \nu_q^c r_q^{c\dagger} r_q^c. \quad (12)$$

The RC mapping involves an enlarged view of a redefined supersystem S' whose self-energy term $H_{S'}(t)$ now incorporates, in addition to the unchanged terms for the self-energy of the TLS, the self-energies for the RC from each reservoir as well as coupling terms between the TLS and each RC. The remaining terms, collected together in $H_{R'_h}$ and $H_{R'_c}$, represent residual environments R'_h and R'_c and their interactions with the relevant RC, which may be treated as Markovian [26, 27].

In the original frame, we characterise the interaction between the TLS and the reservoirs via a spectral density defined for each of the hot and cold interactions as

$$J(\omega) \equiv \sum_k f_k^2 \delta(\omega - \omega_k). \quad (13)$$

Here we have omitted superscripts denoting hot and cold reservoir versions to avoid encumbering our notation. In the cycle computations we shall take the continuum limit for the bath oscillators, and assume the following functional form of the spectral density for each reservoir,

$$J(\omega) = \frac{\alpha\omega\omega_c}{\omega^2 + \omega_c^2}, \quad (14)$$

where α is the coupling strength and ω_c is a cutoff frequency. Finding explicit expressions for the frequencies ν_k and the operators r_k is not necessary because the residual reservoirs are traced out when deriving a master equation for the enlarged system S' . One simply needs to find a functional form in the continuum limit for the spectral density function $\tilde{J}(\nu) \equiv \sum_k g_k^2 \delta(\nu - \nu_k)$, which characterizes the coupling between S' and the residual hot and cold reservoirs, as well as the parameters Ω and λ , such that the Heisenberg equations of motion for operators in the TLS subspace are equivalent in both pictures. Imposing this results in the following equations fully defining the RC mapping for each reservoir: $\Omega = 2\pi\gamma\omega_c$, $\lambda = \sqrt{\pi\alpha\Omega}/2$, and $\tilde{J}(\omega) = \gamma\omega e^{-\omega/\Lambda}$, where $\gamma = \sqrt{\epsilon^2 + \Delta^2}/2\pi\omega_c$ and we eventually take the cutoff frequency Λ to infinity in order to ensure that the original form of spin-boson spectral density is accurately represented post mapping [27].

In order to numerically solve the RC master equation it is necessary to truncate the Hilbert space for the quantum state of the supersystem S' . In practice this means truncating the number of excitations N_{RC} we consider in the RC mode. We choose the truncation such that the engine metrics (in particular the work output of the cycle) are converged.

Whereas in standard treatments of heat engines, one is accustomed to applying the weak coupling assumption such that the quantum state for the total system remains as a tensor product between TLS and reservoir degrees of freedom at all times, here the weak coupling approximation is applied to the residual environments. This results in a total state which is in product form at all times in the degrees of freedom of S' , R'_h and R'_c , namely $\rho_{S'} \otimes \rho_{R'_h} \otimes \rho_{R'_c}$, but where correlations between the TLS and the hot and the cold RC will form and indeed persist even in the limit cycle. These correlations are crucial to the performance of the engine in the finite coupling regime. We show in the following that the resulting coherence in the reduced TLS quantum state leads to a quantum limit to the engine's output which is not present in an incoherent version of the cycle, and cannot be captured by a weak coupling Born-Markov treatment.

B. Rethermalising reservoirs

Standard thermodynamic treatments of the Otto cycle consider thermal reservoir resources. To be consistent with this at strong coupling in the infinite time Otto

cycle, Ref. [28] assumed that if system-reservoir interactions drive a particular reservoir out of equilibrium by the end of an isochore, then by the time the system is coupled once more the reservoir has returned to thermal equilibrium. This is the reason only reservoir decoupling costs are present in Ref. [28] and costs from coupling to a reservoir evaluate to zero. We also wish here to isolate strong coupling effects from any which may be due to coupling to heat reservoirs which are out of thermal equilibrium at the start of each isochore. To this end, we shall include a mechanism in our finite time cycle to ensure that any uncoupled reservoir returns to thermal equilibrium by the time it is coupled once more to the TLS.

Labelling S'_h the enlarged system of TLS plus hot reservoir RC, the master equation governing the dynamics of S'_h during the hot isochore is given by

$$\frac{d\rho(t)}{dt} = L_h[\rho(t)], \quad (15)$$

with

$$L_h[\rho(t)] \equiv -i \left[H_{S'_h}, \rho(t) \right] - [A_h, [\chi, \rho(t)]] + [A_h, \{\Xi, \rho(t)\}], \quad (16)$$

where the first term on the right hand side governs the unitary evolution of S'_h and the other terms induce decoherence and dissipation in the energy eigenbasis of S'_h . Here, we have defined $A_h = a_h + a_h^\dagger$, the self-Hamiltonian $H_{S'_h}$ only includes terms for the hot RC and its interaction with the TLS, and the operators χ and Ξ are given by [27]

$$\chi = \gamma \int_0^\infty d\tau \int_0^\infty d\omega \omega \cos(\omega\tau) \coth\left(\frac{\beta_h\omega}{2}\right) A_h(-\tau), \quad (17)$$

$$\Xi = \gamma \int_0^\infty d\tau \int_0^\infty d\omega \cos(\omega\tau) [H_{S'}, A_h(-\tau)], \quad (18)$$

where $A_h(\tau) \equiv e^{iH_{S'_h}\tau} A_h e^{-iH_{S'_h}\tau}$. The operator $\rho(t)$ represents the state of the TLS plus each reservoir RC and, for ease of notation in Eq. (15), we have omitted identity operators acting on the uncoupled cold reservoir degrees of freedom. We can ensure that the cold reservoir, which has been driven out of equilibrium during the previous cold isochore, returns to thermal equilibrium at temperature T_c while the hot reservoir and TLS interact by adding terms to Eq. (15) which act only on the uncoupled cold RC space and hence do not depend on the full system plus RC eigenstructure. The uncoupled RC is a simple harmonic oscillator so we may add standard weak coupling dissipators which take the following form [32, 33]

$$L_d[\rho] = \gamma_d(N_c + 1) \left\{ a_c \rho a_c^\dagger - \frac{1}{2} a_c^\dagger a_c \rho - \frac{1}{2} \rho a_c^\dagger a_c \right\} + \gamma_d N_c \left\{ a_c^\dagger \rho a_c - \frac{1}{2} a_c a_c^\dagger \rho - \frac{1}{2} \rho a_c a_c^\dagger \right\}. \quad (19)$$

Here, $N_c = e^{-\beta_c \Omega_c} / (1 - e^{-\beta_c \Omega_c})$ is the thermal occupation number for the cold RC with frequency Ω_c at inverse temperature $\beta_c = 1/T_c$. We choose the rate γ_d to ensure thermalisation occurs over a timescale such that the TLS re-couples to a thermal reservoir at the start of the subsequent isochore. The cold isochore may be treated in an analogous fashion by making the replacements $S'_h \rightarrow S'_c$, $A_h \rightarrow A_c$, $a_h \rightarrow a_c$, and $\beta_h \rightarrow \beta_c$ in Eq. (15) as well as the replacements $a_c \rightarrow a_h$ and $N_c \rightarrow N_h$ in the damping terms in Eq. (19), where N_h is the thermal occupation number of the hot RC at inverse temperature $\beta_h = 1/T_h$, i.e. $N_h = e^{-\beta_h \Omega_h} / (1 - e^{-\beta_h \Omega_h})$.

C. Computing out of equilibrium engine states around the Otto cycle

The work output of the Otto cycle is given by the net energy change of the system across each of the isentropic strokes. This also involves accounting for the energetic costs associated with turning off the interaction term at the end of these strokes, leading to the following expression for work output [28]

$$W = \text{tr} [H_S^c \rho^C] - \text{tr} [H_S^h \rho^B] + \text{tr} [H_S^h \rho^A] - \text{tr} [H_S^c \rho^D] - \text{tr} [H_{I_h} \rho^B] - \text{tr} [H_{I_c} \rho^D]. \quad (20)$$

Here, h and c superscripts on the Hamiltonian operators indicate that the splitting in the TLS is set to μ_h and μ_c , respectively. The density operator ρ is labelled with superscripts $A - D$ indicating the various points around the cycle and represents the state of S' , the enlarged system consisting of the TLS and the two RCs.

The first four terms in Eq. (20) are the usual energetic contributions for the work output of the cycle, which arise also in a weak coupling treatment (note that they depend on H_S , the bare TLS Hamiltonian). The final two terms are a distinct feature of the strong coupling treatment and arise because of costs of decoupling the TLS from either the hot or the cold reservoir. Since, as described previously, we include terms which bring about a rethermalisation of the non-interacting RC once it is decoupled, there are no coupling costs [28].

The energy transferred into the system during the hot isochore is given by

$$Q = \text{tr} [H_{S'}^h \rho^B] - \text{tr} [H_{S'}^h \rho^A], \quad (21)$$

and we shall term this heat. Due to the presence of the mapped $H_{S'}$, this expression contains contributions from the interaction energy between the TLS and the RC as well as a contribution from the RC being pulled out of equilibrium. These are neglected in weak coupling treatments but are important at stronger coupling and computable within the RC framework.

To evaluate the net work output, Eq. (20), and the energy transferred into the system during the hot isochore, Eq. (21), one needs to compute the quantum states ρ^{A-D} of the enlarged system S' at each of the points A, B, C

and D when the engine is operating in the limit cycle. In the infinite time (equilibrium) version of the cycle, this involves taking the steady state solution of an enlarged RC master equation of the form of Eq. (15) along each isochore to obtain the states ρ^B and ρ^D . The states ρ^C and ρ^A can be obtained by unitary evolution along the isentropic strokes. For the non-equilibrium case with finite time isochores, the calculation is much more involved and we must solve the dynamical equation of motion for the full state S' for a particular isochore time τ_i . For point B , the equation of motion along the hot isochore is given by

$$\frac{d}{dt} \rho(t) = L_{A' \rightarrow B}[\rho(t)], \quad (22)$$

where $L_{A' \rightarrow B}[\rho(t)] = L_h[\rho(t)] + L_d[\rho(t)]$, see Eqs. (16) and (19). For a particular isochore time τ_i , the solution to this equation is

$$\rho^B = \mathcal{U}_h(\tau_i)[\rho^A] \equiv \exp(L_{A' \rightarrow B} \tau_i)[\rho^A]. \quad (23)$$

Decoupling from the hot reservoirs happens instantaneously and thus the state is unchanged between B and B' .

During the isentropic expansion stroke we tune $\epsilon(t)$ and $\Delta(t)$ such that $(\epsilon_h, \Delta_h) \rightarrow (\epsilon_c, \Delta_c)$ and in such a way that TLS Hamiltonians at different times along the isentrope commute with each other, $[H_S(t), H_S(t')] = 0$. This ensures that the the TLS Hamiltonians at the start of the stroke, $H_S(0)$, and at the end of the stroke at a time we label τ , $H_S(\tau)$, share a common energy eigenbasis. The TLS quantum state in this case adiabatically follows the change in splitting and no coherence develops even when the stroke is carried out in a finite time τ . We thus avoid any quantum friction along the isentropic strokes, and any losses in performance due to the generation of coherence can instead be attributed to the isochores. For the purposes of maximising power output, it is then preferable to complete this stroke quickly and we consider here the limit $\tau \rightarrow 0$. This means the state at point C is unchanged from that at point B' .

The interaction term for the cold bath is turned on instantaneously at this point with no change in the system state and then the subsequent two strokes are carried out completely analogously to the previous two, but with the cold and hot RC terms switching roles during the cold isochore, and with (ϵ_c, Δ_c) and (ϵ_h, Δ_h) exchanging places in the Hamiltonian governing the evolution of the TLS along the subsequent isentropic compression stroke. In general, one complete cycle will return a different state at A' than the state at the start of the cycle. However, after a number of cycles, these transient dynamics vanish and the limit cycle is reached [3], where the state at any one particular point is the same from one cycle to the next. This is the regime in which the engine's figures of merit are computed.

III. RESULTS

A. Non-equilibrium engine metrics

In Fig. 1 we plot the power output and efficiency of the Otto cycle heat engine at finite coupling. The power output initially increases with coupling strength until a turnover is reached and output falls as reservoir decoupling costs begin to dominate over the increase in work output. Note that we are considering here a finite isochore time, τ_i , shorter than that which is necessary for a stationary state to be reached along the isochore (at which point, it is known that work output always decreases with coupling strength [28]). The energy absorbed from the hot reservoir increases with coupling strength too and this leads to an engine efficiency which decreases monotonically with coupling strength. However, the metric one often seeks to improve upon in practice is the power output, and we see here that at finite coupling before costs begin to dominate, there is a region where it is beneficial to increase the system-reservoir coupling.

A similar finding is also reflected in the analysis of the strong coupling regime for a heat engine in Ref. [34] but there the isochores are long enough that the engine is considered to have reached arbitrarily close to equilibrium. In the present case, we show that in fact power output can be maximised before this equilibrium has been reached in Fig. 2. Here we plot the behaviour of the work and power outputs as a function of the isochore time τ_i for an intermediate coupling strength. As the system S' approaches equilibrium, the work output saturates. Power output, however, is maximised before the working system has reached its equilibrium. If the desired metric for the engine is how much power it can produce, it is thus preferable for it to operate out of equilibrium, by choosing shorter isochore times and intermediate coupling strengths.

An Otto cycle heat engine outputs an optimal amount of work when it is permitted to absorb the maximum amount of heat during the hot isochore and convert this into work adiabatically along the hot isentropic stroke. For the process to be cyclic, some energy must be dissipated into a colder reservoir and some work done on the working system before it is brought back into contact with the hot reservoir once more. Performing the isochoric strokes in finite time means that a less than maximal amount of heat can be exchanged between the working system and the reservoirs, with the consequent effect that a less than optimal amount of net work is performed by the engine. However, in reality engines are designed to operate out of equilibrium in order that they may generate a finite amount of power. There is therefore a tradeoff to be had between extracting as much work as possible, and reducing the amount of time needed to perform a cycle.

Increasing the interaction strength between the TLS and the reservoirs in this engine speeds up the process

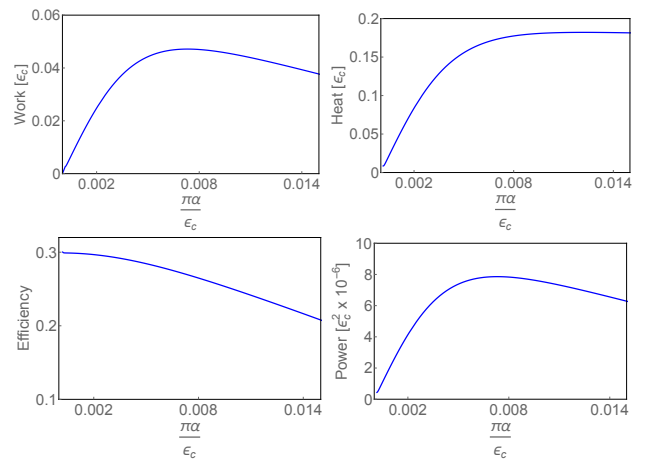


FIG. 1. Work output (top left), heat absorbed (top right), efficiency (bottom left) and power output (bottom right) of the non-equilibrium TLS Otto cycle engine, each as a function of coupling strength $\pi\alpha/\epsilon_c$ for $\epsilon_c\tau_i = 3000$. Parameters: $\epsilon_h = 1.5\epsilon_c$, $\Delta_c = \epsilon_c$, $\Delta_h = 1.5\epsilon_c$, $\omega_c = 0.265\epsilon_c$, $\epsilon_c\beta_h = 0.95$, $\epsilon_c\beta_c = 2.5$, $N_{RC} = 9$. We see that work output and power increase with coupling strength up to a point where interaction costs begin to dominate and subsequently reverse this trend. The heat absorbed from the hot reservoir increases with coupling strength. Efficiency monotonically decreases with coupling strength.

of equilibration. The closer the TLS is permitted to get to its eventual equilibrium state before embarking on the isentropic strokes, the more heat is absorbed (or dissipated) during the hot (or cold) isochore. This then translates into a larger population difference between the two energy eigenlevels of the TLS during the isentropic strokes, which is desired for optimal work extraction. Increasing the coupling strength is therefore one way of mitigating the loss in work output by performing the isochoric strokes in finite time. The penalty one has to pay is an energetic cost due to system-reservoir decoupling because at stronger coupling the TLS pulls the reservoirs out of equilibrium. But for intermediate coupling strengths, before these costs begin to dominate too severely, the time saved along the isochores translates into a greater power output at stronger coupling.

B. Quantum nature of the heat engine

We wish to isolate the effects on engine performance of system-reservoir correlations accrued during the (heat exchange) isochoric strokes as a result of finite coupling with the reservoirs. These correlations manifest themselves in finite coherences in the working system state. We shall therefore make a distinction between a fully quantum version of the cycle where system-reservoir correlations lead to quantum coherence being generated along the isochores, and one where coherence is prevented from accumulating. In this latter version of the cycle, we introduce into Eq. (15) terms that induce pure dephas-

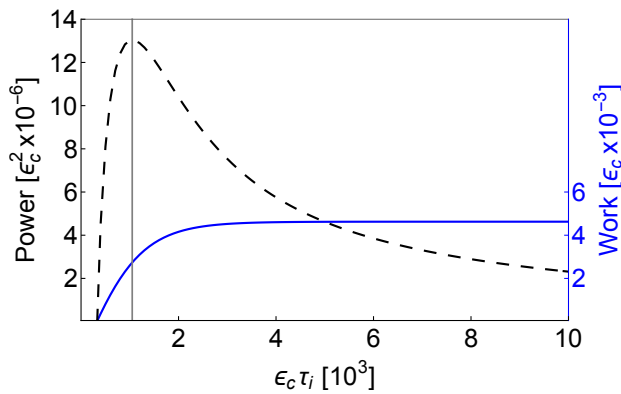


FIG. 2. A joint plot of power and work against isochore time for $\alpha = 0.01\epsilon_c/\pi$, with work plotted in blue on the right hand axis and power plotted in black dashed on the left hand axis. Parameters: $\epsilon_h = 1.5\epsilon_c$, $\Delta_c = \epsilon_c$, $\Delta_h = 1.5\epsilon_c$, $\omega_c = 0.265\epsilon_c$, $\epsilon_c\beta_h = 0.95$, $\epsilon_c\beta_c = 2.5$, $N_{RC} = 9$. We see that power is maximised at isochore times that are shorter than those required for the engine to have equilibrated (where work output saturates).

ing [32, 35–37] in the energy eigenbasis of the working system, while taking care that these have no energetic contribution to the overall evaluation of work output or energy exchange with the reservoirs. To meet with this latter criteria, these purely dephasing terms must commute with the mapped Hamiltonian $H_{S'}$, which we diagonalise and write as

$$H_{S'} = \sum_n E_n |E_n\rangle \langle E_n|. \quad (24)$$

We then construct a purely dephasing Liouvillian term as

$$L_{dep}[\rho(t)] = \gamma_{dep} \sum_n \left[|E_n\rangle \langle E_n|, [|E_n\rangle \langle E_n|, \rho(t)] \right]. \quad (25)$$

We are free to choose the numerical value of γ_{dep} to ensure dephasing occurs on an appropriate timescale, such that coherence is prevented from developing during the isochoric strokes of the engine. We can then compute the states of the working system at various points around the cycle as previously described, but with the addition of these terms to $L_{A' \rightarrow B}$ and $L_{C' \rightarrow D}$ acting on S'_h in the former and on S'_c in the latter. We define the incoherent engine as the version of the cycle where these pure dephasing terms have been included during the isochoric strokes. We stress that these terms achieve pure dephasing in the energy eigenbasis of the enlarged TLS plus RC (i.e. $H_{S'}$) rather than just the TLS energy eigenbasis. This is the natural choice for a system interacting strongly with an environment. Introducing pure dephasing terms into the master equation that only act on the TLS would be inappropriate since they do not commute with the unitary part of the master equation, which depends on $H_{S'}$, and as such they have a non-zero energetic contribution.

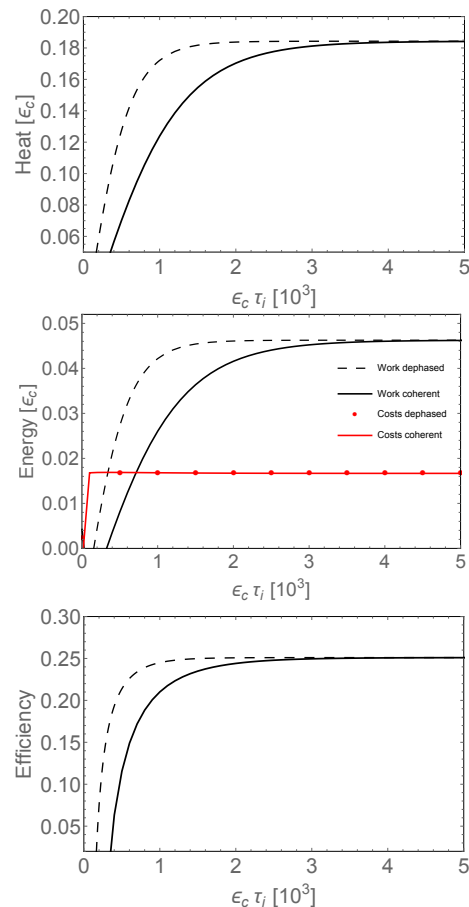


FIG. 3. Heat (top), work and decoupling costs (middle), and efficiency (bottom) plotted against isochore time $\epsilon_c \tau_i$ for the non-equilibrium TLS Otto cycle. Solid curves represent the fully coherent engine while dotted curves depict the behaviour of the incoherent engine where quantum coherence has been suppressed by pure dephasing in the energy eigenbasis of S' . Parameters: $\alpha = 0.01\epsilon_c/\pi$, $\epsilon_h = 1.5\epsilon_c$, $\Delta_c = \epsilon_c$, $\Delta_h = 1.5\epsilon_c$, $\omega_c = 0.265\epsilon_c$, $\epsilon_c\beta_h = 0.95$, $\epsilon_c\beta_c = 2.5$, $N_{RC} = 9$. We see that dephasing leads to a quicker approach to equilibrium values for heat, work output, and therefore efficiency. Decoupling costs remain comparable in both types of engine.

We compare these two versions of the Otto cycle, coherent and incoherent, and analyse the effect of quantum coherence on engine performance in Fig. 3 as a function of isochore time. The solid curves depict the behaviour of the fully coherent engine, while the dotted curves represent the incoherent version of the cycle. At longer isochore times, i.e. larger τ_i , the incoherent and coherent engines converge. Here, the state of S' approaches thermal equilibrium with the relevant residual reservoir which is maintained at the hot or cold temperature. This state is then diagonal in the energy eigenbasis of S' , and so no coherence is present in either type of engine at points B or D if the isochore is long enough. For shorter times, however, this is not the case, and pure dephasing does have an appreciable effect on the engine metrics.

The dephased engine absorbs more heat along the hot

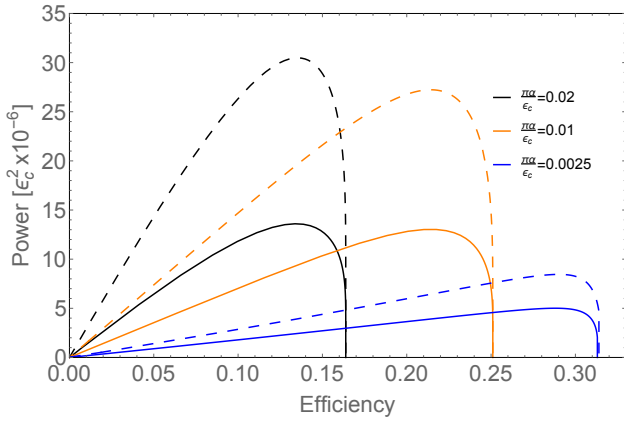


FIG. 4. Parametric plot of power output against efficiency for the non-equilibrium TLS Otto cycle for various values of coupling strength α . Solid curves represent the fully coherent engine while dotted curves depict the behaviour of the incoherent engine. The parameter which is varied along the curves is the isochore time τ_i . Other parameters: $\epsilon_h = 1.5\epsilon_c$, $\Delta_c = \epsilon_c$, $\Delta_h = 1.5\epsilon_c$, $\omega_c = 0.265\epsilon_c$, $\epsilon_c\beta_h = 0.95$, $\epsilon_c\beta_c = 2.5$, $N_{RC} = 9$. We see that dephasing in the energy eigenbasis of S' leads to an engine that outperforms its quantum coherent counterpart for a range of coupling strengths. At weaker coupling, this effect is less dramatic but still pronounced.

isochore but outputs a net work large enough to compensate for this, yielding a higher efficiency than the fully coherent engine. Decoupling costs remain comparable. These are dominated by the RC state being driven out of equilibrium along the isochores, which is not prevented by dephasing terms. In Fig. 4 we show this improved engine performance in parametric plots of power versus efficiency when varying the isochore time, for a selection of coupling strengths. Even at weaker but finite coupling, where coherence generation is less severe, an improvement in power and efficiency over the coherent engine can be achieved by dephasing.

In a traditional weak coupling treatment of the Otto cycle the TLS equilibrates to a Gibbs state for long isochore times, which is diagonal in the energy eigenbasis. This is a probabilistic distribution of energy eigenstates and involves no quantum coherence. With the isentropic strokes carried out adiabatically, populations in these energy eigenstates are kept constant and no coherence in the working system state accumulates. In fact, if the isentropic strokes remain adiabatic when the cycle is treated at finite time (as we consider), then no coherence is present during the cycle at any time. At non-negligible system-reservoir interaction strengths, however, correlations that are generated between the TLS and the reservoir lead to quantum coherence in the energy eigenbasis at the end of the isochores. This coherence will, in general, persist during the isentropic strokes even if they are performed adiabatically. In this way, the strongly coupled TLS Otto cycle is inherently quantum in nature.

We illustrate how dephasing in the TLS plus RC basis accelerates the process of equilibration of the working

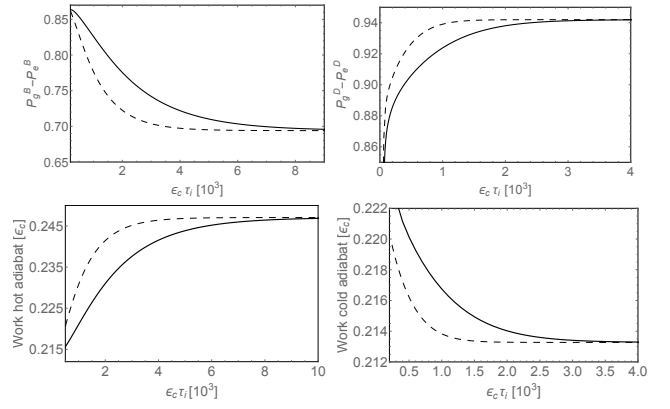


FIG. 5. The difference in population of the TLS eigenstates at point B in the Otto cycle, just before the hot adiabatic stroke (top left), the difference in population of the TLS eigenstates at point D, just before the cold adiabatic stroke (top right), work extracted during the hot adiabatic stroke (bottom left) and work input during the cold adiabatic stroke (bottom right), each plotted against isochore time τ_i . Solid curves represent the fully coherent engine while dotted curves depict the behaviour of the incoherent engine. Parameters: $\alpha = 0.01\epsilon_c/\pi$, $\epsilon_h = 1.5\epsilon_c$, $\Delta_c = \epsilon_c$, $\Delta_h = 1.5\epsilon_c$, $\omega_c = 0.265\epsilon_c$, $\epsilon_c\beta_h = 0.95$, $\epsilon_c\beta_c = 2.5$, $N_{RC} = 9$. We see that dephasing in the energy eigenbasis of S' leads to a population difference at crucial points around the cycle that is more beneficial for net work extraction. At shorter isochore times, there is a smaller population difference at point B in the version of the engine where coherence has been suppressed, meaning more heat has been absorbed during the hot isochore and more work can be extracted on the subsequent stroke. At point D, there is a larger population difference in the dephased engine, meaning more heat has been dumped into the cold reservoir during the cold isochore, and less work is done on the subsequent stroke.

system S' in Fig. 5. Of crucial importance for heat and work calculations, which result from average energy variations between the points of the Otto cycle, are the differences in ground and excited state populations of the TLS in the eigenbasis of H_S . In Fig. 5 we show how these are affected by dephasing in the full TLS plus RC energy eigenbasis at point B, just before the hot adiabatic stroke begins, and at point D, just before the cold adiabatic stroke begins.

For longer isochore times, the population difference at points B and D is the same in both the fully coherent and dephased (incoherent) engines, hence the engine metrics are the same for both types. At shorter times, the dephased engine displays a faster approach to the steady state than the fully coherent engine. At point B there is therefore a smaller population difference (top left) at shorter τ_i and at point D a larger population difference (top right). This results in greater work extracted during the hot adiabat (bottom left) and smaller work invested during the cold adiabat (bottom right) for the dephased engine.

At point B, we wish to have as much population as possible in the excited state and therefore as small a population difference as possible, the limiting case be-

ing that of infinite temperature with half the population in the ground state and half in the excited state. The smaller the population difference at point B therefore, the higher the (effective) temperature reached by the TLS. This entails that more heat has been absorbed from the hot reservoir during the hot isochore and that the subsequent hot adiabatic stroke can extract a larger amount of work. We recall that this stroke is carried out adiabatically (in the sense that the Hamiltonian commutes at all times) and the population difference in the TLS is preserved up to point C.

At point D, after interacting with the cold reservoir, it is desirable to have as little population in the excited state as possible and therefore as large a population difference as possible. This corresponds to a low temperature (recall that the ground state is the theoretical thermal state with zero temperature). It means that as much heat as possible has been dissipated into the cold reservoir and that on the subsequent adiabatic stroke, the work performed on the system can be kept to a minimum.

IV. DISCUSSION

A quantum system undergoing an Otto cycle in any practical application operates in a regime not typically considered in theoretical descriptions (see Refs. [34, 38] for recent exceptions): that of finite coupling and finite time. Our analysis here shows that maximising power output for completing whatever task the engine may be designed for in a realistic time can be achieved by manipulating the coupling strength. This is limited by the work costs a finite system-reservoir interaction entails and schemes to mitigate this cost, such as those described in Ref [28], are suggested as an avenue for further investigation.

The increase in power output results directly from the reduction in the time it takes for the working system to absorb and dissipate heat into the reservoirs, an effect which is not purely quantum in nature. However, our comparison of a distinctly quantum version of the Otto cycle with one where quantum effects are minimized has shown that, at finite coupling, the working system develops coherence in the energy eigenbasis at finite isochore times as a result of correlations with the environment. This coherence limits the power output of the engine. Schemes to dephase this coherence are therefore a promising avenue of research for mitigating this quantum disadvantage and optimising the population difference between the working system energy eigenstates for work extraction.

This is a distinct effect from that of quantum friction, which degrades the work extraction strokes of quantum heat engines when these strokes are carried out in non-adiabatic conditions. Our results highlight that even when the engine operates in an adiabatic regime where there are no non-adiabatic transitions during the work strokes and hence no quantum friction, quantum coherence enters the cycle through finite system-reservoir interactions.

Finite coupling results in a natural basis for the working system that is dressed by a collective degree of freedom from the environment with which it is interacting. Results not presented here, obtained by considering the effect of dephasing in the reduced TLS energy eigenbasis alone, indicate that the behaviour of such a stochastic engine is qualitatively similar to the case presented here; engine performance can be enhanced. However, dephasing in the TLS energy eigenbasis is also problematic. When included in a master equation for the enlarged system S' , purely dephasing terms on the TLS subsystem can lead to unphysical population differences at the end of the isochores. This issue arises because terms which induce pure dephasing on the TLS in a weak coupling master equation have a different effect in the enlarged RC master equation. They can also act to change the population difference in the TLS since they do not commute with the enlarged system self-Hamiltonian $H_{S'}$, which includes a coupling term between the system and the RC. These terms therefore also entail an undesired energetic contribution (leading to the erroneous population differences).

It has been shown that finite reservoir coupling is detrimental to the performance of infinite time heat engine cycles when compared to cases in which the coupling strength is vanishingly weak [28]. This is due primarily to the energetic costs imposed when decoupling the working system and reservoirs around the cycle in the finite coupling case. Our focus here has been markedly different. Instead of comparing weak with strong coupling only, we have focussed on the relative performance of coherent and incoherent heat engine cycles where both are operating at finite coupling strength. We conclude by stressing that strong system-reservoir coupling imposes a uniquely quantum coherent limit on heat engine performance which is not captured by standard weak coupling Born-Markov approaches.

Acknowledgments— We thank Luis Correa for discussions. D.N. is supported by the Engineering and Physical Sciences Research Council and the Centre for Doctoral Training in Controlled Quantum Dynamics. F.M. is supported by ERC Grant ODYCQUENT. A.N. is supported by the Engineering and Physical Sciences Research Council Grant No. EP/N008154/1.

[1] R. Alicki, Journal of Physics A: Mathematical and General **12**, L103 (1979).

[2] R. Kosloff, J. Chem. Phys. **80**, 1625 (1984).

[3] Y. Rezek and R. Kosloff, New J. Phys. **8**, 83 (2006).

- [4] H. T. Quan, Y.-X. Liu, C. P. Sun, and F. Nori, Phys. Rev. E **76**, 031105 (2007).
- [5] N. Linden, S. Popescu, and P. Skrzypczyk, Phys. Rev. Lett. **105**, 130401 (2010).
- [6] J. Roßnagel, O. Abah, F. Schmidt-Kaler, K. Singer, and E. Lutz, Phys. Rev. Lett. **112**, 030602 (2014).
- [7] R. Kosloff and A. Levy, Annual Review of Physical Chemistry **65**, 365 (2014).
- [8] P. Skrzypczyk, A. J. Short, and S. Popescu, Nature Commun. **5** (2014).
- [9] L. A. Correa, J. P. Palao, G. Adesso, and D. Alonso, Phys. Rev. E **87**, 042131 (2013).
- [10] D. Gelbwaser-Klimovsky, W. Niedenzu, and G. Kurizki, Advances In Atomic, Molecular, and Optical Physics **64**, 329 (2015).
- [11] D. Gelbwaser-Klimovsky and A. Aspuru-Guzik, J. Phys. Chem. Lett. **6**, 3477 (2015).
- [12] P. P. Hofer and B. Sothmann, Phys. Rev. B **91**, 195406 (2015).
- [13] P. P. Hofer, J.-R. Souquet, and A. A. Clerk, Phys. Rev. B **93**, 041418 (2016).
- [14] R. Kosloff and T. Feldmann, Phys. Rev. E **65**, 055102 (2002).
- [15] J. Pekola, B. Karimi, and G. Thomas, arXiv:1812.10933 (2018).
- [16] M. V. Berry, Journal of Physics A: Mathematical and Theoretical **42**, 365303 (2009).
- [17] E. Torrontegui, S. Ibáñez, S. Martínez-Garaot, M. Modugno, A. del Campo, D. Guéry-Odelin, A. Ruschhaupt, X. Chen, and J. G. Muga, in *Advances in Atomic, Molecular, and Optical Physics*, Vol. 62, edited by E. Arimondo, P. R. Berman, and C. C. Lin (Academic Press, 2013).
- [18] T. Feldmann and R. Kosloff, Phys. Rev. E **73**, 025107 (2006).
- [19] R. Uzdin, A. Levy, and R. Kosloff, Phys. Rev. X **5**, 031044 (2015).
- [20] R. Uzdin, A. Levy, and R. Kosloff, Entropy **18** (2016).
- [21] K. Brandner, M. Bauer, and U. Seifert, Phys. Rev. Lett. **119**, 170602 (2017).
- [22] J. Roßnagel, S. T. Dawkins, K. N. Tolazzi, O. Abah, E. Lutz, F. Schmidt-Kaler, and K. Singer, Science **352**, 325 (2016).
- [23] B. Karimi and J. P. Pekola, Phys. Rev. B **94**, 184503 (2016).
- [24] J. Klatzow, J. N. Becker, P. M. Ledingham, C. Weinzetl, K. T. Kaczmarek, D. J. Saunders, J. Nunn, I. A. Walmisley, R. Uzdin, and E. Poem, Phys. Rev. Lett. **122**, 110601 (2019).
- [25] A. Nazir and G. Schaller, *The Reaction Coordinate Mapping in Quantum Thermodynamics*. In: Binder F., Correa L., Gogolin C., Anders J., Adesso G. (eds) *Thermodynamics in the Quantum Regime. Fundamental Theories of Physics*, Vol. 195 (Springer, 2019).
- [26] J. Iles-Smith, A. G. Dijkstra, N. Lambert, and A. Nazir, J. Chem. Phys. **144**, 044110 (2016).
- [27] J. Iles-Smith, N. Lambert, and A. Nazir, Phys. Rev. A **90**, 032114 (2014).
- [28] D. Newman, F. Mintert, and A. Nazir, Phys. Rev. E **95**, 032139 (2017).
- [29] P. Strasberg, G. Schaller, N. Lambert, and T. Brandes, New J. Phys. **18**, 073007 (2016).
- [30] G. Schaller, J. Cerrillo, G. Engelhardt, and P. Strasberg, Phys. Rev. B **97**, 195104 (2018).
- [31] R. Kosloff and Y. Rezek, Entropy **19**(4), 136 (2017).
- [32] H.-P. Breuer and F. Petruccione, *The theory of open quantum systems* (Oxford University Press, Oxford, 2002).
- [33] H. Carmichael, *Statistical methods in quantum optics: master equations and Fokker-Planck equations* (Springer, New York, 1999).
- [34] M. Perarnau-Llobet, H. Wilming, A. Riera, R. Gallego, and J. Eisert, Phys. Rev. Lett. **120**, 120602 (2018).
- [35] M. A. Schlosshauer, *Decoherence and the quantum-to-classical transition* (Springer, Berlin, 2007).
- [36] D. G. Tempel and A. Aspuru-Guzik, Chemical Physics **391**, 130 (2011).
- [37] P. Rebentrost, M. Mohseni, I. Kassal, S. Lloyd, and A. Aspuru-Guzik, New J. Phys. **11**, 033003 (2009).
- [38] M. Wiedmann, J. T. Stockburger, and J. Ankerhold, arXiv:1903.11368 (2019).